Journal of the Neurological Sciences 385 (2018) 22–29

Contents lists available at ScienceDirect

Journal of the Neurological Sciences

journal homepage: www.elsevier.com/locate/jns

Extrastriatal degeneration correlates with deficits in the motor domain subscales of the UHDRS

Victor Galvez[a,b,h], Gabriel Ramírez-García[b], Carlos R. Hernandez-Castillo[c], Leo Bayliss[d], Rosalinda Díaz[e], María Margarita Lopez-Titla[f], Aurelio Campos-Romo[b], Juan Fernandez-Ruiz[a,e,g,*]

[a] Instituto de Neuroetología, Universidad Veracruzana, Mexico
[b] Unidad Periférica de Neurociencias, Facultad de Medicina, Universidad Nacional Autónoma de México, Instituto Nacional de Neurología y Neurocirugía "MVS", Mexico
[c] CONACYT - Instituto de Neuroetología, Universidad Veracruzana, Mexico
[d] Instituto Nacional de Neurología y Neurocirugía "Manuel Velasco Suarez", Mexico
[e] Laboratorio de Neuropsicología, Departamento de Fisiología, Facultad de Medicina, Universidad Nacional Autónoma de México, Mexico
[f] Imágenes Cerebrales, Servicios Clínicos, Instituto Nacional de Psiquiatría "Ramón de la Fuente Muñiz", Mexico
[g] Facultad de Psicología, Universidad Veracruzana, Mexico
[h] Universidad Panamericana, Escuela de Psicología, Laboratorio de Neurociencias cognitivas y desarrollo, Mexico

ARTICLE INFO

Keywords:
Huntington's disease
Voxel-based morphometry
UHDRS
MRI
Basal ganglia

ABSTRACT

Introduction: Striatal degeneration has significant behavioral effects in patients with Huntington's disease (HD). However, there is scant evidence of the possible contribution of extrastriatal regions to the motor alterations assessed within the different domains of the Unified Huntington's Disease Rating Scale (UHDRS).
Objective: Analyze if extrastriatal grey matter decrease in patients with HD correlates with motor performance assessed with the UHDRS and its different domains.
Method: Twenty-two molecular diagnosed patients with incipient HD, and twenty-two control participants matched for sex and age participated in this study. Voxel-based morphometry (VBM) analyses were done to identify grey matter decrease in the HD patients, and its relationship with the motor deterioration measured with the UHDRS motor scale. To further explore this relationship, a principal component analysis (PCA) was done on the UHDRS domains scores. Then the average of each component was used as a covariate in a VBM analysis. Finally, individual sub-scores from each domain were also tested for correlations with the VBM results.
Results: In addition to the striatal degeneration, the VBM analysis showed significant negative correlations between the global UHDRS scores and the cerebellum, insula and precuneus atrophy. The UHDRS PCA showed component-related negative correlations suggesting a specific impact of individual degenerations. Further analyses with the individual sub-scores showed more specific corelations, including: chorea, with right caudate and left posterior cingulate gyrus; ocular pursuit, with left precentral gyrus, left superior temporal gyrus, cerebellum culmen and right temporal lobe. Saccadic movements with left postcentral gyrus and left middle occipital gyrus.
Conclusion: In the early stages of HD, it is possible to find correlations between behavioral alterations as measured with the UHDRS motor domains, and extrastriatal regions, including specific areas of the cerebellum, and insular, parietal and frontal cortices. These areas could contribute to the HD related impairments along with the classical deficits associated with the striatal degeneration.

1. Introduction

Atrophy in the bilateral striatum in early Huntington's Disease (HD) has been identified using Voxel-based morphometry (VBM) [23]. Neurodegeneration in the caudate, as measured with VBM, in HD has been correlated negatively with motor, cognitive and psychiatric symptoms [5,11,13]. However, the caudate nucleus is not the only structure of the basal ganglia that has been correlated with behavioral measures of HD severity. For instance, globus pallidus and thalamus degeneration have been correlated negatively with scores from the Total Functional Capacity scale (TFC), which measures involve occupation, finances, activities of daily living and care level [5]. Aside from the basal ganglia, other structures have also been implicated in HD, including the possible effect of cerebellar atrophy on motor and

* Corresponding author at: Departamento de Fisiología, Facultad de Medicina, Universidad Nacional Autónoma de México, UNAM, Coyoacán 04510, Mexico.
E-mail address: jfr@unam.mx (J. Fernandez-Ruiz).

https://doi.org/10.1016/j.jns.2017.11.040
Received 19 October 2016; Received in revised form 29 June 2017; Accepted 30 November 2017
Available online 01 December 2017
0022-510X/

psychiatric deficits [14].

Clinically, the motor functions in patients with HD are mainly assessed using the Unified Huntington's Disease Rating Scale (UHDRS) [10]. This scale evaluates the performance in a variety of motor domains, including: ocular pursuit movements and saccades, orolingual performance, motor programming, dystonia, chorea and gait. Although the scale has an undisputed clinical value, it is unfortunate that most imaging studies analyzing the possible correlations between motor dysfunction and neuronal degeneration only use the total UHDRS motor score as a covariate. This approach has precluded a better understanding of the possible relationship between different brain areas and scores on specific domains of the UHDRS scale, including the potential contribution of the extrastriatal areas that could be related to specific behaviors measured in each domain of the UHDRS.

Therefore, using the VBM technique, we tested whether motor alterations in the different UHDRS domains are related to decreases over distinct or overlapping brain areas. We evaluated a group of patients with early HD using T1-weighted 3D structural magnetic resonance images (MRI), and compared them with age-matched controls. Then, we analyzed the relationship between brain atrophy and the UHDRS global scores, the results of a principal component analysis (PCA) averaged components, and the UHDRS individual domains from each component.

2. Method

2.1. Participants

Twenty-two patients with HD, confirmed with molecular diagnosis, and twenty-two healthy participants age and sex matched to the HD group, participated in this study (Table 1 for demographics). The healthy volunteers self-reported no history of neurological or psychiatric disorders. All the procedures were performed according to the Declaration of Helsinki [28] and approved by health and ethics committees of the Instituto Nacional de Neurología y Neurocirugía "MVS" and the Universidad Nacional Autónoma de México.

The patients with HD had incipient clinical manifestations according to the scores obtained with the TFC scale and the UHDRS motor scale [10]. After acquiring the UHDRS motor scale, the subscores were fed into a PCA to extract the main components using varimax rotation with a Kaiser normalization.

Table 1
Participant demographics.

	Ctrl	HD
Male:Female	9:13	9:13
Age (years)	45 ± 13	45.6 ± 12.1
CAG repeat length	–	44.3 ± 3.9
Duration of symptoms (years)	–	4.3 ± 3
TFC		11.7 ± 1.8
Disease burden		385.6 ± 100.3
UHDRS motor scale: global score	–	14.6 ± 10.6
UHDRS motor scale: chorea score	–	3.3 ± 3.7
UHDRS motor scale: ocular pursuit score	–	1.4 ± 1.6
UHDRS motor scale: saccadic movements score	–	2.8 ± 2.7
UHDRS motor scale: dysarthria	–	0.4 ± 0.5
UHDRS motor scale: tongue protrusion	–	0.2 ± 0.5
UHDRS motor scale: finger taps	–	1.7 ± 1.1
UHDRS motor scale: pronate/supinate-hands	–	0.6 ± 0.9
UHDRS motor scale: Luria	–	0.6 ± 0.7
UHDRS motor scale: rigidity-arms	–	0.8 ± 0.9
UHDRS motor scale: bradykinesia-body	–	0.6 ± 0.7
UHDRS motor scale: maximal dystonia	–	1.4 ± 2.4
UHDRS motor scale: gait	–	0.5 ± 0.7
UHDRS motor scale: tandem walking	–	0.9 ± 1.1
UHDRS motor scale: retropulsion pull test	–	1 ± 1.5

All the patients with HD were scored according to the components of the UHDRS motor scale, whose range is 0 to 128 and higher scores reflect a greater motor impairment. The highest scores obtained by our patients were in the items: oculomotor pursuit, saccade initiation, saccade velocity, maximal chorea and maximal dystonia. In the Total Functional Capacity Scale (TFC), 11 to 13 scores are defined as the Stage I of the disease. The values represent the mean ± standard deviation.

2.1.1. Image acquisition

All images were acquired using a 3.0 Tesla Achieva MRI scanner (Phillips medical Systems, Eindhoven, The Netherlands) at the Instituto Nacional de Psiquiatría "Ramon de la Fuente Muñiz" in Mexico City. The high-resolution anatomical acquisition consisted of a 3-D_T1 Fast Field-Echo sequence with TR/TE of 8/3.7 ms, FOV of 256 × 256 mm, an acquisition and reconstruction matrix of 256 × 256, resulting in isometric resolution of 1 × 1 × 1 mm.

2.1.2. Voxel-based morphometry

Grey matter volume (GMV) measurements were performed using VBM analysis [1] with FSL (FMRIB Software Library) [21]. First, voxels that did not represent cerebral tissue were excluded through BET software. The resulting images were segmented into grey matter, white matter, and cerebrospinal fluid. The images corresponding to the grey matter from all participants were aligned to Neurological Institute of Montreal MNI152 standard space by means of a nonlinear co-registration. The average of these co-registered images was obtained to generate an HD specific template for this study. In a secondary step, the individual grey matter images were co-registered to this specific template through a non-linear co-registration, and local changes in expansion or contraction were corrected through a process known as modulation [8]. Smoothing was applied with a Gaussian isotropic kernel with a sigma of 3 mm. Using the FSL randomize tool [27] a Two-sample *t*-test was performed between the HD group and controls. Significant degeneration was defined as voxels with a p-value < 0.01.

The associations between grey matter density and the motor deficits in patients with HD were examined using analysis of covariance (ANCOVA). Three different analyses were run. In the first analysis, FSL randomize was fed with the global UHDRS scores. The second analyses used the mean score of each of the resulting UHDRS motor scale PCA components: Component 1, composed by dysarthria, pronate/supinate-hands, maximal dystonia, bradykinesia-body, maximal chorea, finger taps, tongue protrusion and gait; Component 2, composed by rigidity-arms, ocular pursuit and retropulsion test; Component 3, composed by saccade movements and tandem walking; Component 4, Luria. Finally, in the third analysis, scores from the individual domains were tested (Table 1).

All the analyses were corrected using the Threshold-Free Cluster Enhancement analysis (TFCE) with 10,000 randomized permutations [9]. Also, to avoid bias on the multiple comparisons, and as the rotated component matrix showed four independent components, the threshold selected by Bonferroni correction to each domain was 0.01, considering $\alpha = 0.05$. For all the analyses, the disease burden score (calculated using the formula: age × [CAG repeat length − 35.5]) was included as nuisance variable.

Finally, the voxels local maxima *t*-values were used to perform Pearson's correlation analyses between the grey matter density from those regions and the respective behavioral scores, using the Statistical Package for the Social Sciences software (SPSS version 23, Chicago, Illinois, USA). To perform this correlation analysis, the dependent variable was the grey matter density values from each patient, obtained from 4D multi-subject concatenated and smoothed images (GM_mod_merg_s3 file in FSL) and, the independent variable, were the scores obtained by each patient.

3. Results

3.1. HD related grey matter atrophy

The VBM analysis showed a significant GMV decrease in the HD

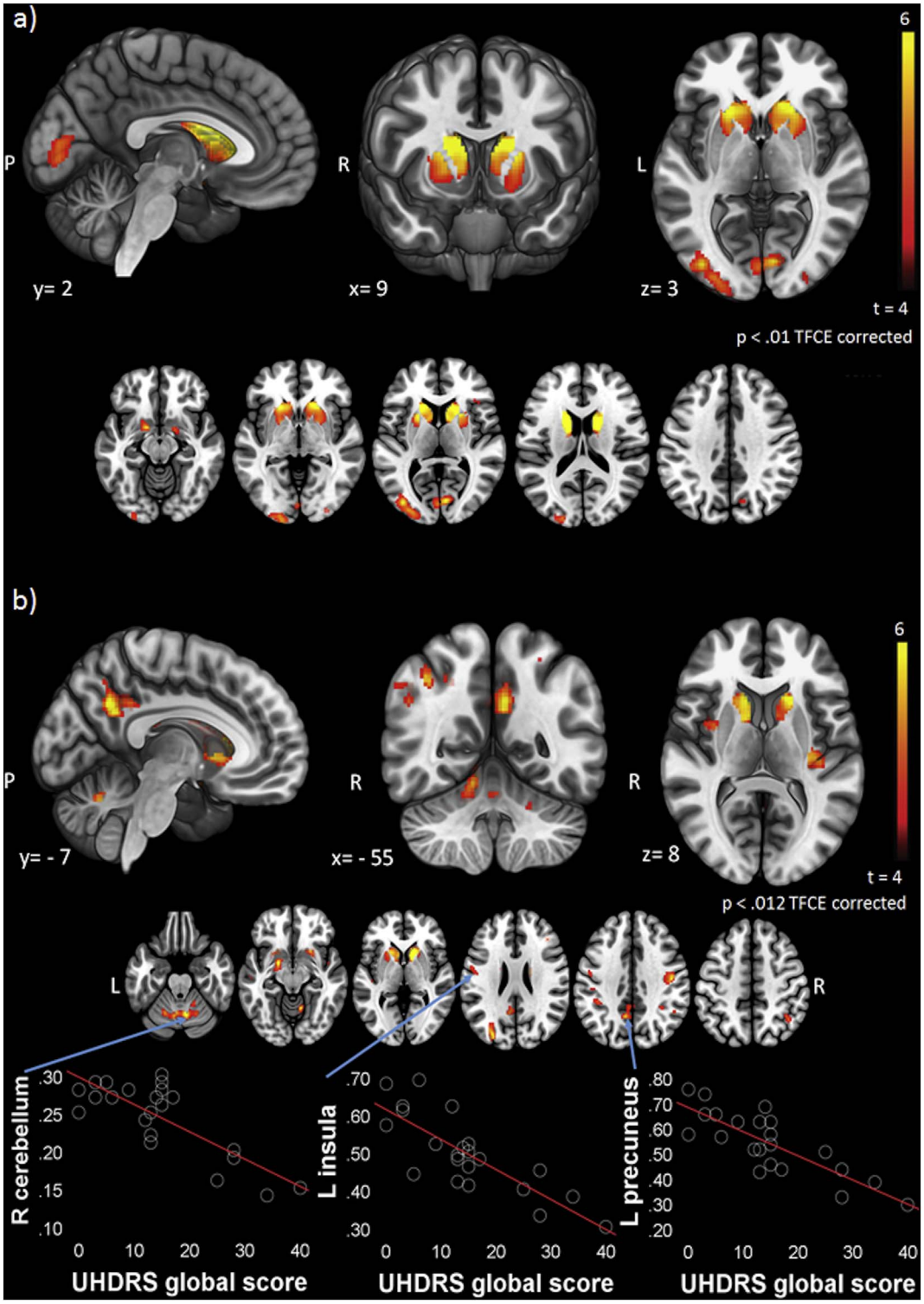

Fig. 1. Voxel-based morphometry analysis. a) Comparison between control and Huntington's disease groups. The t-scores are indexed by the color bar indicating the brain regions showing significant grey matter decrease in patients compared with controls. b) Significant associations between grey matter volume and UHDRS scores in HD patients. Color maps indicate the FSL randomize t-score of each association. All the analyses were corrected by TFCE, significant p-value < 0.012. Scatter plots show the Pearson's correlation between the indicated cluster with the voxel local maxima and the corresponding score. P, posterior; R, right; L, left.

group, including in the bilateral caudate, putamen, bilateral precuneus and left occipital middle gyrus (Fig. 1a).

3.2. VBM correlations with the global UHDRS scores

The total scores from the UHDRS motor scale correlated with the GMV decrease in striatal regions in the bilateral caudate and left putamen. The global UHDRS scores also correlated negatively with several extrastriatal regions, including the right cerebellum, right precentral gyrus and precuneus, insula, and middle occipital gyrus from the left hemisphere (Fig. 1b, Table 3).

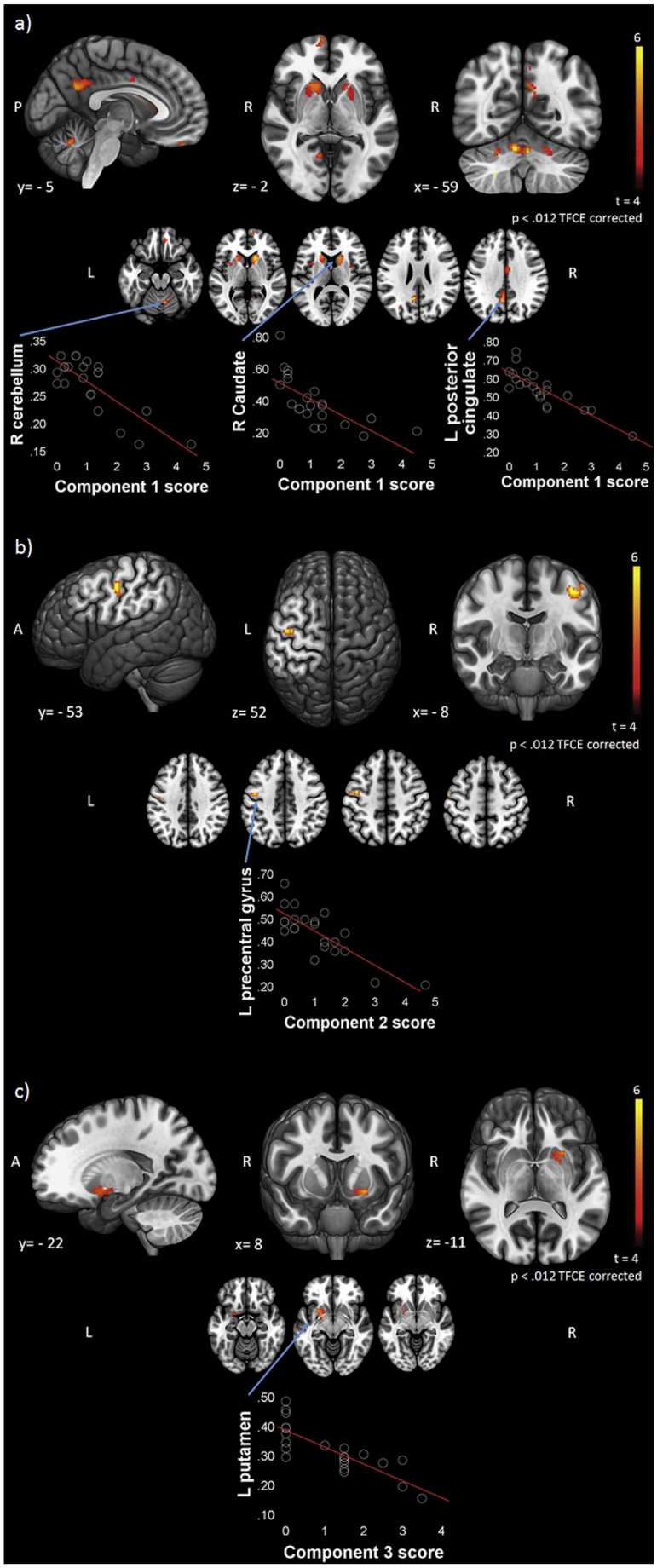

Fig. 2. Scores from the three principal components extracted by factorial analysis in the UHDRS scores, examined using analysis of covariance: a) Component 1; b) Component 2; c) Component 3. Color maps indicate the FSL randomize t-score of each association. All the analyses were corrected by TFCE, significant p-value $<$ 0.012. Scatter plots show the Pearson's correlation between the indicated cluster with the voxel local maxima and the corresponding score. P, posterior; A; anterior; R, right; L, left.

Table 2
Anatomical regions that show correlation between grey matter volume and principal components extracted by factorial analysis in the UHDRS scores.

Anatomical region	MNI coordinates (mm)			*t*-values	Cluster size	Pearson	R^2	*p*
	x	*y*	*z*					
Component 1								
R caudate	14	20	4	5.7	493	− 0.709	0.503	0.00002
L posterior cingulate	− 6	− 56	28	7.15	229	− 0.844	0.712	0.00008
R inferior parietal lobe	40	− 54	50	6.54	23	− 0.833	0.694	0.00000
R cerebellum culmen	6	− 62	− 22	6.4	112	− 0.804	0.646	0.00000
L caudate	− 18	18	10	5.3	257	− 0.665	0.442	0.001
Component 2								
L precentral gyrus	− 42	− 8	48	6.8	111	− 0.809	0.655	0.00000
Component 3								
L putamen	− 26	10	− 10	5.6	143	− 0.811	0.657	0.00000

3.3. VBM correlations with the principal component from UHDRS scores

The mean scores for each component resulting from PCA correlated negatively with GMV decrease. The Component 1 correlated with bilateral caudate nucleus, bilateral cerebellum, right inferior parietal lobe and left posterior cingulate gyrus. The Component 2 correlated with left precentral gyrus. The Component 3 correlated with left putamen. Finally, the Component 4 did not show any GMV correlation (Fig. 2, Table 2).

3.4. VBM correlations with the sub-scores of the UHDRS domains

The analyses from the sub-scores of each component showed specific correlations. The chorea scores correlated negatively with GMV decrease in the right caudate nucleus. Outside the basal ganglia, they correlated with the precuneus and portion of the left posterior cingulate gyrus (Fig. 3a, Table 3). The ocular pursuit scores, showed mainly correlation with extrastriatal regions including left precentral gyrus, left superior temporal gyrus and right cerebellum (Fig. 3b, Table 3). Finally, the scores from saccadic movements showed a relationship with GMV decrease in extrastriatal regions including postcentral gyrus and middle occipital gyrus from left hemisphere; however, did not show a correlation with any striatal region (Fig. 3c, Table 3). The VBM analysis did not show additional significant correlations between other components sub-scores and grey matter atrophy in the patients with HD.

4. Discussion

In this study, we explored if the GMV of extrastriatal and striatal regions correlated with the scores from the UHDRS in patients with HD. Our results confirm our hypothesis that early global motor alterations in patients with incipient HD did correlate negatively with both striatal and extrastriatal regional decreases, including the right cerebellum, precuneus, insula, middle occipital gyrus, and precentral gyrus, of the left hemisphere. Furthermore, our results show correlations between individual domains of the UHDRS scale, and neurodegeneration of specific regions of the brain, including extrastriatal areas.

4.1. UHDRS global analysis

The VBM analysis used to explore grey matter loss revealed a number of regions, including striatal and extrastriatal areas that showed significant GMV decreases in patients with HD. Other regions included the bilateral caudate, right precentral gyrus, putamen, precuneus, and precentral middle occipital gyrus from left hemisphere, which are consistent with the classic neuropathophysiology described in early HD stages [26], and with previous VBM findings showing widespread cerebral pathology in early HD [15,23].

The manifestation of motor alterations in patients with HD has traditionally been considered a consequence of neuronal loss in the striatum [12,23]. Thus, our correlational analyses identified, as expected, significant relationships between the total scores from the UHDRS motor scale and the GMV decrease in striatal regions, including the left putamen and caudate bilaterally, confirming previous studies [5,22]. However, our results show that the global motor alterations in patients did correlate not only with GMV decreases in the striatum, but also with the cerebellum, precuneus, insula, cingulate gyrus, middle occipital gyrus and precentral gyrus. Similar to our findings, other studies have also found results showing a correlation between the GMV in extrastriatal areas and deficits in the motor and cognitive domains in HD [3,17,19]. Furthermore, the areas found to correlate with the global scores have been previously associated with behavioral and cognitive deficits in HD, including the cerebellum [18], the cingulate [24], the precuneus, the precentral gyrus, and the middle occipital gyrus [16].

4.2. UHDRS motor domains analysis

The analysis of the possible relationship between the components obtained from the PCA analysis and the reduction in grey matter resulted in different correlation patterns. For example, significant correlations with the caudate head and putamen, are shown for the first component, but not for the second, suggesting that degeneration of specific areas contribute to deficits in different components of the UHDRS.

Further analyses also found correlations between UHDRS motor domains sub-scales and specific brain areas. As far as we know, this has not been explored before. In addition to the caudate nucleus, our analyses found that GMV in the posterior cingulate gyrus correlated negatively with the patient's chorea scores. These results are partly supported by previous PET findings showing deficits in the cingulate and premotor cortex during movements in patients with HD [4], suggesting that, besides the striatum, cortical degeneration could play a role in the increase of HD chorea.

Regarding the ocular pursuit domain, significant correlations were found with the right cerebellum, consistent with previous studies in healthy participants that have found that Purkinje cells activity in the ventral paraflocculus correlates with eyes velocity and acceleration [20]. Correlations were also found with the left superior temporal gyrus, which has been associated with visual search and spatial perception [7]. Also, as expected, significant correlations were found with the frontal eye fields in the middle frontal gyrus, and with the caudate, which is consistent with previous findings related to oculomotor abnormalities in HD [19].

Finally, the saccadic movements UHDRS domain scores correlated with the left middle occipital gyrus, which has been involved in cortical target direction and modulation of voluntary saccades [2]. Supporting previous findings, our results also showed that saccadic movements also correlated with the left parietal lobe, which is involved in visuospatial integration and in reflexive saccade triggering [6,25].

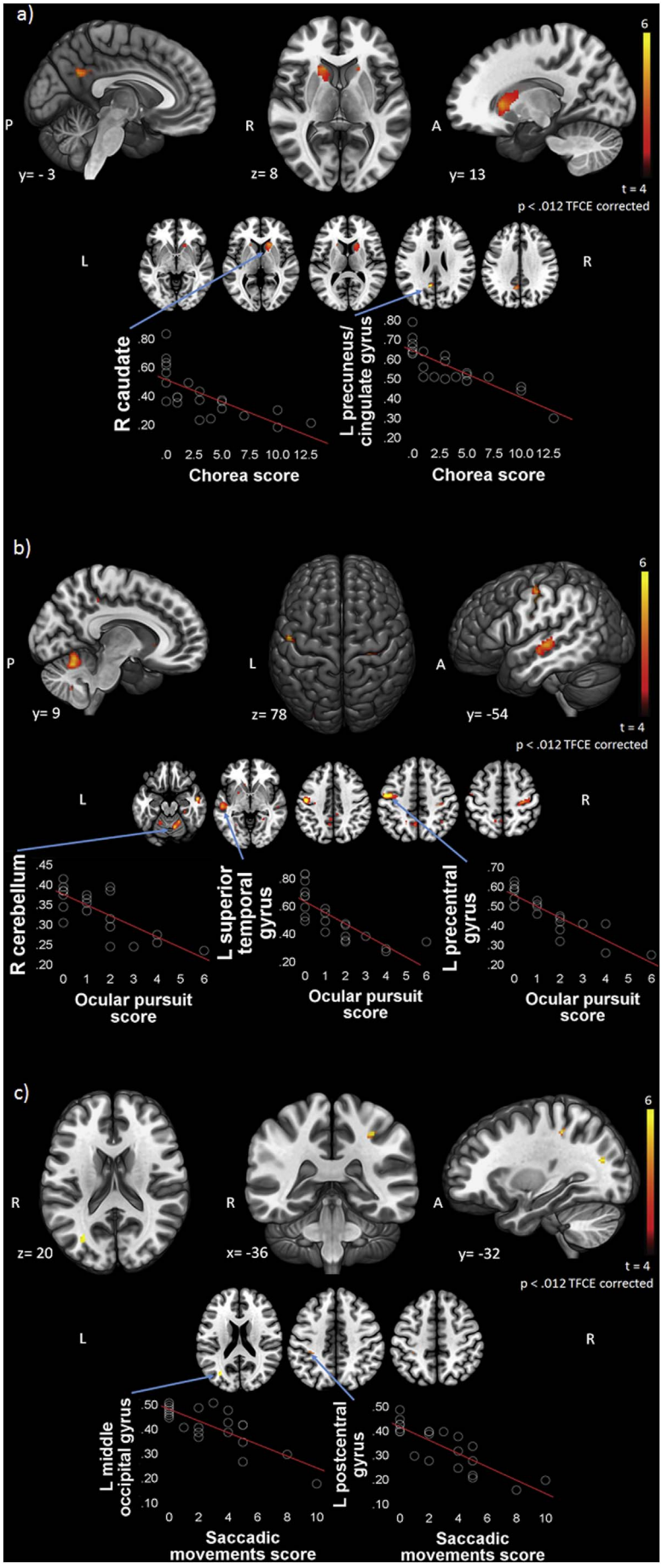

Fig. 3. Significant associations between grey matter volume and UHDRS scores in HD patients: a) UHDRS chorea scores; b) UHDRS ocular pursuit scores; c) Saccadic movements scores. Color maps indicate the FSL randomize t-score of each association. All the analyses were corrected by TFCE and the subdomain scores also by Bonferroni method, significant p-value < 0.012. Scatter plots show the Pearson's correlation between the indicated cluster with the voxel local maxima and the corresponding score. P, posterior; A; anterior; R, right; L, left.

Table 3
Anatomical regions that show correlation between grey matter volume and UHDRS motor score.

Anatomical region	MNI coordinates (mm)			*t*-values	Cluster size	Pearson	R^2	*p*
	x	*y*	*z*					
UHDRS global scores								
R caudate	12	14	0	7.3	326	− 0.806	0.649	0.00000
L caudate	− 16	20	10	6.4	148	− 0.750	0.563	0.00005
R cerebellum	8	− 62	− 22	7.5	467	− 0.796	0.634	0.00000
L insula	− 36	− 20	8	5.8	163	− 0.811	0.658	0.00000
L middle occipital gyrus	− 30	− 80	24	5.9	189	− 0.806	0.649	0.00000
R precentral gyrus	46	− 14	38	5.8	167	− 0.801	0.641	0.00000
L precuneus	− 8	− 56	34	6.5	315	− 0.818	0.669	0.00000
L putamen	− 22	14	− 10	5.2	9	− 0.745	0.654	0.00007
UHDRS chorea scores								
R caudate	16	20	4	5.3	28	− 0.701	0.492	0.00020
L precuneus/posterior cingulate gyrus	− 6	− 56	28	6.8	43	− 0.830	0.689	0.00000
UHDRS ocular pursuit scores								
L precentral gyrus 4	− 48	− 10	46	8.4	154	− 0.884	0.781	0.00050
R cerebellum culmen	18	− 50	− 22	5.8	13	− 0.765	0.595	0.00003
L superior temporal gyrus	− 54	− 22	− 2	5.4	2	− 0.775	0.600	0.00002
R temporal lobe	52	− 6	− 20	5.5	21	− 0.787	0.620	0.00001
UHDRS saccadic movements scores								
L postcentral gyrus	− 32	− 36	46	6.6	15	− 0.830	0.689	0.00000
L middle occipital gyrus	− 32	− 72	20	6.6	8	− 0.794	0.631	0.00004

5. Conclusions

Our results showed correlations of UHDRS motor domain specific with a decrease in distinct extrastriatal areas in patients with incipient HD. These results suggest that using only the global UHDRS motor score as a motor impairment variable could dampen the efforts to define the brain areas compromised with the clinical assessment of HD. We suggest that future imaging studies assessing HD degeneration should include the UHDRS individual domain scores in their volumetric or functional analyses.

Funding agencies

This study was supported in part by: CONACYT grant No. 220871 and PAPIIT-UNAM grant No. IN214716 to JFR and CONACYT Ph.D. scholarship No. 369794 to VG.

Special thanks to M. D. María de Lourdes Martínez Gudiño, head of Department of Brain Imaging, from Instituto Nacional de Psiquiatría “Ramón de la Fuente Muñiz”, for all facilities offered for carrying out imaging studies.

References

[1] J. Ashburner, K.J. Friston, Voxel-based morphometry—the methods, NeuroImage 11 (6) (2000) 805–821, http://dx.doi.org/10.1006/nimg.2000.0582.
[2] S.V. Astafiev, C.M. Stanley, G.L. Shulman, M. Corbetta, Extrastriate body area in human occipital cortex responds to the performance of motor actions, Nat. Neurosci. 7 (5) (2004) 542–548, http://dx.doi.org/10.1038/nn1241.
[3] F.A. Barrios, L. Gonzalez, R. Favila, M.E. Alonso, P.M. Salgado, R. Diaz, J. Fernandez-Ruiz, Olfaction and neurodegeneration in HD, Neuroreport 18 (1) (2007) 73–76, http://dx.doi.org/10.1097/WNR.0b013e3280102302.
[4] P. Bartestein, A. Weind, S. Spiengel, et al., Central motor processing in Huntington's disease. A pet study, Brain 120 (1997) 1553–1567, http://dx.doi.org/10.1093/brain/120.9.1553.
[5] G. Douaud, V. Gaura, M.J. Ribeiro, F. Lethimonnier, R. Maroy, C. Verny, ... P. Remy, Distribution of grey matter atrophy in Huntington's disease patients: a combined ROI-based and voxel-based morphometric study, NeuroImage 32 (4) (2006) 1562–1575, http://dx.doi.org/10.1016/j.neuroimage.2006.05.057.
[6] B. Gaymard, C.J. Ploner, S. Rivaud, A.I. Vermersch, C. Pierrot-Deseilligny, Cortical control of saccades, Exp. Brain Res. 123 (1–2) (1998) 159–163, http://dx.doi.org/10.1002/ana.410370504.
[7] A. Gharabaghi, M.F. Berger, M. Tatagiba, H.O. Karnath, The role of the right superior temporal gyrus in visual search—insights from intraoperative electrical stimulation, Neuropsychologia 44 (12) (2006) 2578–2581, http://dx.doi.org/10.1016/j.neuropsychologia.2006.04.006.
[8] C.D. Good, I.S. Johnsrude, J. Ashburner, R.N. Henson, K.J. Fristen, R.S. Frackowiak, A voxel-based morphometric study of ageing in 465 normal adult human brains, Biomedical Imaging, 2002, 5th IEEE EMBS International Summer School on (pp. 16-pp.), IEEE, June, 2002, , http://dx.doi.org/10.1006/nimg.2001.0786.
[9] S. Hayasaka, T.E. Nichols, Combining voxel intensity and cluster extent with permutation test framework, NeuroImage 23 (1) (2004) 54–63.
[10] Huntington Study Group, Unified Huntington's Disease Rating Scale: Reliability and Consistency, (1996), http://dx.doi.org/10.1002/mds.870110204.
[11] D. Joel, Open interconnected model of basal ganglia-thalamocortical circuitry and its relevance to the clinical syndrome of Huntington's disease, Mov. Disord. 16 (3) (2001) 407–423, http://dx.doi.org/10.1002/mds.1096.
[12] M.J. Novak, S.J. Tabrizi, Huntington's disease, BMJ 340 (2010), http://dx.doi.org/10.1136/bmj.c3109.
[13] A. Peinemann, S. Schuller, C. Pohl, T. Jahn, A. Weindl, J. Kassubek, Executive dysfunction in early stages of Huntington's disease is associated with striatal and insular atrophy: a neuropsychological and voxel-based morphometric study, J. Neurol. Sci. 239 (1) (2005) 11–19, http://dx.doi.org/10.1016/j.jns.2005.07.007.
[14] E.M. Rees, R. Farmer, J.H. Cole, S. Haider, A. Durr, B. Landwehrmeyer, R. Scahill, S. Tabrizi, N.Z. Hobbs, Cerebellar abnormalities in Huntington's disease: a role in motor and psychiatric impairment? Mov. Disord. 29 (13) (2014) 1648–1654, http://dx.doi.org/10.1002/mds.25984.
[15] H.D. Rosas, et al., Evidence for more widespread cerebral pathology in early HD: an MRI-based morphometric analysis, Neurology 60 (10) (2003) 1615–1620, http://dx.doi.org/10.1212/WNL.62.3.523-a.
[16] H.D. Rosas, N.D. Hevelone, A.K. Zaleta, D.N. Greve, D.H. Salat, B. Fischl, Regional cortical thinning in preclinical Huntington disease and its relationship to cognition, Neurology 65 (5) (2005) 745–747, http://dx.doi.org/10.1212/01.wnl.0000174432.87383.87.
[17] H.D. Rosas, D.H. Salat, S.Y. Lee, A.K. Zaleta, V. Pappu, B. Fischl, ... S.M. Hersch, Cerebral cortex and the clinical expression of Huntington's disease: complexity and heterogeneity, Brain 131 (4) (2008) 1057–1068, http://dx.doi.org/10.1093/brain/awn025.
[18] U. Rüb, F. Hoche, E.R. Brunt, H. Heinsen, K. Seidel, D. Del Turco, ... H.W. Korf, Degeneration of the cerebellum in Huntington's disease (HD): possible relevance for the clinical picture and potential gateway to pathological mechanisms of the disease process, Brain Pathol. 23 (2) (2013) 165–177, http://dx.doi.org/10.1111/j.1750-3639.2012.00629.x.
[19] R.I. Scahill, N.Z. Hobbs, M.J. Say, N. Bechtel, S. Henley, H. Hyare, ... A. Durr, Clinical impairment in premanifest and early Huntington's disease is associated with regionally specific atrophy, Hum. Brain Mapp. 34 (3) (2013) 519–529, http://dx.doi.org/10.1002/hbm.21449.
[20] Shidara, M., Kawano, K., Gomi, H., & Kawato, M. (1993). Inverse-dynamics model eye movement control by Purkinje cells in the cerebellum. doi: https://doi.org/10.1038/365050a0.
[21] S.M. Smith, M. Jenkinson, M.W. Woolrich, C.F. Beckmann, T.E. Behrens, H. Johansen-Berg, R.K. Niazy, Advances in functional and structural MR image analysis and implementation as FSL, NeuroImage 23 (2004) S208–S219, http://dx.doi.org/10.1016/j.neuroimage.2004.07.051.
[22] S.J. Tabrizi, R.I. Scahill, A. Durr, R.A. Roos, B.R. Leavitt, R. Jones, ... C. Kennard, Biological and clinical changes in premanifest and early stage Huntington's disease in the TRACK-HD study: the 12-month longitudinal analysis, Lancet Neurol. 10 (1) (2011) 31–42, http://dx.doi.org/10.1016/S1474-4422(10)70276-3.
[23] M.J. Thieben, A.J. Duggins, C.D. Good, L. Gomes, N. Mahant, F. Richards, E. McCusker, R.S.J. Frackowiak, The distribution of structural neuropathology in pre-clinical Huntington's disease, Brain 125 (8) (2002) 1815–1828, http://dx.doi.org/10.1093/brain/awf179.

[24] D.C. Thu, D.E. Oorschot, L.J. Tippett, A.L. Nana, V.M. Hogg, B.J. Synek, ... R.L. Faull, Cell loss in the motor and cingulate cortex correlates with symptomatology in Huntington's disease, Brain 133 (4) (2010) 1094–1110, http://dx.doi.org/10.1093/brain/awq047.

[25] I. Vaca-Palomares, B.C. Coe, D.C. Brien, D.P. Munoz, J. Fernandez-Ruiz, Voluntary saccade inhibition deficits correlate with extended white-matter cortico-basal atrophy in Huntington's disease, NeuroImage Clin. (2017), http://dx.doi.org/10.1016/j.nicl.2017.06.007.

[26] J.P. Vonsattel, R.H. Myers, T.J. Stevens, R.J. Ferrante, E.D. Bird, E.P. Richardson Jr., Neuropathological classification of Huntington's disease, J. Neuropathol. Exp. Neurol. 44 (6) (1985) 559–577, http://dx.doi.org/10.1097/00005072-198511000-00003.

[27] A.M. Winkler, G.R. Ridgway, M.A. Webster, S.M. Smith, T.E. Nichols, Permutation inference for the general linear model, NeuroImage 92 (2014) 381–397, http://dx.doi.org/10.1016/j.neuroimage.2014.01.060.

[28] World Medical Association, Bulletin of the World Health Organization, 794 (2001), p. 373, http://dx.doi.org/10.1001/jama.2013.281053.